IR photodissociation spectroscopy of $(OCS)_n^+$ and $(OCS)_n^-$ cluster ions: Similarity and dissimilarity in the structure of CO_2, OCS, and CS_2 cluster ions

Yoshiya Inokuchi[a)] and Takayuki Ebata
Department of Chemistry, Graduate School of Science, Hiroshima University, Higashi-Hiroshima, Hiroshima 739-8526, Japan

Infrared photodissociation (IRPD) spectra of $(OCS)_n^+$ and $(OCS)_n^-$ ($n = 2–6$) cluster ions are measured in the 1000–2300 cm^{-1} region; these clusters show strong CO stretching vibrations in this region. For $(OCS)_2^+$ and $(OCS)_2^-$, we utilize the messenger technique by attaching an Ar atom to measure their IR spectra. The IRPD spectrum of $(OCS)_2^+Ar$ shows two bands at 2095 and 2120 cm^{-1}. On the basis of quantum chemical calculations, these bands are assigned to a C_2 isomer of $(OCS)_2^+$, in which an intermolecular semi-covalent bond is formed between the sulfur ends of the two OCS components by the charge resonance interaction, and the positive charge is delocalized over the dimer. The $(OCS)_n^+$ ($n = 3–6$) cluster ions show a few bands assignable to "solvent" OCS molecules in the 2000–2080 cm^{-1} region, in addition to the bands due to the $(OCS)_2^+$ ion core at ~2090 and ~2120 cm^{-1}, suggesting that the dimer ion core is kept in $(OCS)_{3-6}^+$. For the $(OCS)_n^-$ cluster anions, the IRPD spectra indicate the coexistence of a few isomers with an OCS^- or $(OCS)_2^-$ anion core over the cluster range of $n = 2–6$. The $(OCS)_2^-Ar$ anion displays two strong bands at 1674 and 1994 cm^{-1}. These bands can be assigned to a C_s isomer with an OCS^- anion core. For the $n = 2–4$ anions, this OCS^- anion core form is dominant. In addition to the bands of the OCS^- core isomer, we found another band at ~1740 cm^{-1}, which can be assigned to isomers having an $(OCS)_2^-$ ion core; this dimer core has C_2 symmetry and ^2A electronic state. The IRPD spectra of the $n = 3–6$ anions show two IR bands at ~1660 and ~2020 cm^{-1}. The intensity of the latter component relative to that of the former one becomes stronger and stronger with increasing the size from $n = 2$ to 4, which corresponds to the increase of "solvent" OCS molecules attached to the OCS^- ion core, but it suddenly decreases at $n = 5$ and 6. These IR spectral features of the $n = 5$ and 6 anions are ascribed to the formation of another $(OCS)_2^-$ ion core having C_{2v} symmetry with $^2B_2$ electronic state. © *2015 AIP Publishing LLC.* [http://dx.doi.org/10.1063/1.4921991]

I. INTRODUCTION

The charge distribution in molecular cluster ions is one of fundamental properties related to the charge carrier or charge transportation in condensed phase, and it is governed by physical and chemical properties of molecules such as ionization energy (IE), proton affinity (PA), electron affinity (EA), and substituent effects. For homo-dimer radical ions, it is often seen that the intermolecular charge resonance interaction occurs in them, giving a symmetrical species; the charge is equally shared by the two components.[1–19] The dimer ion form is kept as a dimer ion core in some homo-molecular cluster ions, such as $(benzene)_n^+$.[13,14] However, the charge distribution of cluster ions is not predictable so easily on the basis of IE, PA, or EA. One curious manner on the charge distribution occurs for $(CO_2)_n^-$ cluster anions,[16,20,21] which show switching of the ion core between $n = 6$ and 7 and between 13 and 14. The investigation of radical cluster ions in the gas phase has been mainly performed by mass spectrometry, photoelectron spectroscopy, and photodissociation spectroscopy via electronic transitions,

sometimes with the aid of theoretical calculations, in the last few decades. More recently, infrared photodissociation (IRPD) spectroscopy was applied to cluster radical ions; it not only gives the information on the electronic structure, or the charge distribution on the clusters, but also on their geometric structures. Johnson and coworkers reported IRPD spectroscopy of the $(CO_2)_n^-$ cluster anions in the 2300–3800 cm^{-1} regions; in the IR spectra, the bands corresponding to CO_2^- monomer and $(CO_2)_2^-$ dimer cores were clearly observed.[20] In our group, we have been using IRPD spectroscopy to examine static and dynamic behaviors of the positive charge in aromatic cluster radical ions,[22–24] and in cluster radical ions consisting of triatomic molecules such as CO_2, H_2O, CS_2, and N_2O.[25–32] Sanov and coworkers reported an IRPD spectroscopic work of $(CS_2)_2^-$ using a temperature-controlled ion trap and a free electron laser.[33]

In the present study, we extend our IRPD experiments to $(OCS)_n^+$ and $(OCS)_n^-$ cluster ions, in a series of our studies for cluster ions of triatomic molecules.[27,28] For the $(OCS)_n^+$ clusters, the thermochemical stability of the $(OCS)_2^+$ dimer ion was studied by using a pulsed electron-beam high-pressure mass spectrometer, and the formation of a semi-covalent bond in the $(OCS)_2^+$ dimer was reported.[34] The OCS anion clusters have

---

a)Author to whom correspondence should be addressed. Electronic mail: y-inokuchi@hiroshima-u.ac.jp

been much more investigated than the cation clusters, because the $(OCS)_n^-$ clusters are homologous systems of $(CO_2)_n^-$ and $(CS_2)_n^-$, which have complicated but interesting natures of the electronic structure.[16,20,21,33,35–45] Sanov and coworkers have extensively studied photochemistry and electronic structure of $(OCS)_n^-$ using photodissociation and photoelectron imaging techniques.[36–38] They suggested the coexistence of isomers having the OCS^- monomer core and the $(OCS)_2^-$ dimer one. In this study, we apply IRPD spectroscopy to the $(OCS)_n^+$ and $(OCS)_n^-$ cluster ions. The IRPD spectra are measured in the 1000–2300 cm^{-1} region. In order to assign IR bands and determine the cluster structure, we carry out geometry optimization and vibrational analysis of several ion species at the B3LYP/6-311+G* level. Finally, we discuss the similarity and dissimilarity in the structure for the OCS, CO_2, and CS_2 cluster ions.

II. EXPERIMENTAL AND COMPUTATIONAL

The details of our experiment have been given elsewhere.[27] A gas mixture of OCS (0.1%) and Ar is injected into a source chamber through a pulsed nozzle (General Valve Series 9) with an orifice diameter of 0.8 mm at a stagnation pressure of 0.4 MPa. The pulsed free jet crosses an electron beam (350 eV) at the exit of the nozzle, producing the $(OCS)_n^+$, $(OCS)_n^+Ar$, $(OCS)_n^-$, and $(OCS)_n^-Ar$ clusters. Cluster ions produced are accelerated into a flight tube by applying pulsed electric potential (~1.3 kV) to Wiley-McLaren type acceleration grids. By changing the polarity of the acceleration potential, we can select cation or anion clusters. In the flight tube, parent ions of interest are selected with a mass gate. After passing through the gate, mass-selected parent ions are merged with an output of a pulsed IR laser. Resulting fragment ions are mass-analyzed by a home-made reflectron mass spectrometer and detected by a multichannel plate (MCP). Yields of fragment ions are normalized by the intensity of parent ions and the photodissociation laser. IRPD spectra of parent ions are obtained by plotting normalized yields of fragment ions against wavenumber of the IR laser. The fragmentation channel detected for the IRPD spectra of $(OCS)_n^+$ and $(OCS)_n^-$ ($n = 3$–6) is the loss of one OCS molecule. In the case of the $(OCS)_2^+Ar$ and $(OCS)_2^-Ar$ clusters, the IRPD spectra are measured by detecting the Ar loss channel. For the IR laser in the 1000–2300 cm^{-1} region, difference frequency generation (DFG) is obtained by mixing a signal and an idler output of an optical parametric oscillator (OPO) (LaserVision) with an AgGaSe$_2$ crystal. The DFG output is introduced to the vacuum chamber after removing the signal and idler outputs with a ZnSe filter. The output energy is 0.2–1 mJ/pulse with a repetition rate of 10 Hz in the 1000–2300 cm^{-1} region.

In order to analyze the IRPD spectra, we also carry out density functional theory (DFT) calculations with GAUSSIAN03 program package.[46] Geometry optimization and vibrational analysis of $(OCS)_2^+$ and $(OCS)_2^-$ are done at the B3LYP/6-311+G(d) level of theory. For comparison of the IRPD spectra with calculated ones, we employ a scaling factor of 0.9689 to vibrational frequencies calculated. This factor is determined so as to reproduce the frequency of the CO stretching vibration of neutral OCS monomer.[47]
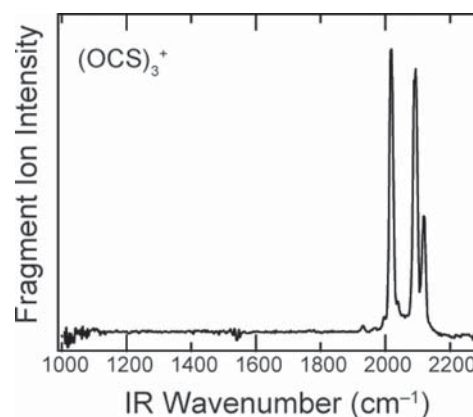
FIG. 1. The IRPD spectrum of the $(OCS)_3^+$ ion in the 1000–2300 cm^{-1} region.

III. RESULTS AND DISCUSSION

A. $(OCS)_n^+$

Figure 1 shows the IRPD spectrum of the $(OCS)_3^+$ ion in the 1000–2300 cm^{-1} region. Strong IR bands are observed in the 1900–2200 cm^{-1} region. These bands can be assigned to CO stretching vibrations, because these band positions are close to that of the CO stretching band of neutral OCS (2050.5 cm^{-1}).[47] Figure 2(a) displays the IRPD spectra of the $(OCS)_2^+Ar$ and $(OCS)_n^+$ ($n = 3$–6) ions in the 1950–2150 cm^{-1} region. For the IR spectrum of the $(OCS)_2^+$ complex, we perform the messenger technique by using the $(OCS)_2^+Ar$ ion.[31] The $(OCS)_2^+Ar$ ion has two bands at 2095 and 2120 cm^{-1}. For the $(OCS)_3^+$ ion, in addition to two band maxima at ~2090 and ~2120 cm^{-1}, one strong band is observed at 2020 cm^{-1}. The IRPD spectra of the $(OCS)_n^+$ ($n = 4$–6) clusters also show two bands around 2090 and
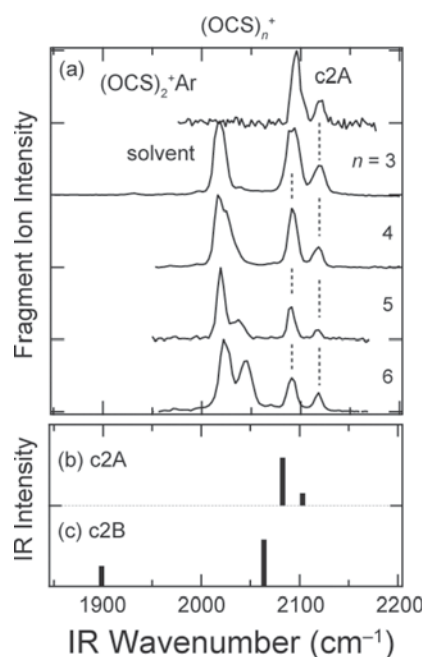
FIG. 2. (a) The IRPD spectra of the $(OCS)_2^+Ar$ and $(OCS)_n^+$ ($n = 3$–6) ions in the CO stretching region. ((b) and (c)) The IR spectra calculated for geometry-optimized structures of $(OCS)_2^+$. A scaling factor of 0.9689 is employed for the calculated vibrational frequencies.
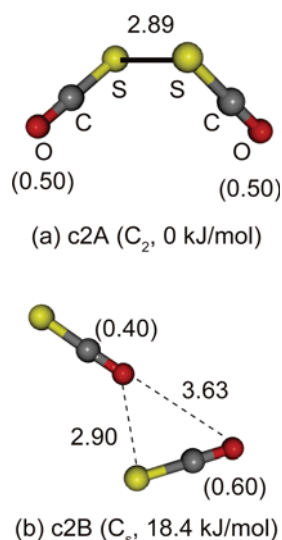
FIG. 3. Optimized structures of the $(OCS)_2^+$ ion. Numbers in the figure show interatomic distances in Å unit. Numbers in parentheses are the Mulliken charge distribution on the constituent molecules. The energy values show the total energy relative to that of the most stable form (c2A). The values are corrected by the zero-point vibrational energy.

2120 cm^{-1} and a few bands in $2000-2070$ cm^{-1}. Thus, all the cluster ions have two bands at ~ 2090 and ~ 2120 cm^{-1}. The intensity of the bands in $2000-2070$ cm^{-1} relative to that of the ~ 2090 and ~ 2120 cm^{-1} bands increases with increasing the cluster size.

In order to assign the IRPD bands of the $(OCS)_2^+Ar$ ion, we perform geometry optimization and the vibrational analysis of the $(OCS)_2^+$ ion at the B3LYP/6-311+G(d) level of theory. Figure 3 shows the optimized structures of the $(OCS)_2^+$ ion (c2A and c2B); the IR spectra calculated for these isomers are displayed in Figs. 2(b) and 2(c). In isomer c2A, which belongs to C_2 point group, an intermolecular bond is formed between the sulfur atoms, and the dihedral angle of the C–S–S–C atoms is calculated to be 98.8°. The positive charge in isomer c2A is equally shared by the two OCS components. Isomer c2B has a planar C_s structure; 60% of the positive charge is localized on one OCS component, and the other one is bonded to it by pointing the oxygen end. Isomer c2A is more stable than c2B by 18.4 kJ/mol. As seen in Fig. 2, the IR spectrum calculated for isomer c2A reproduces the two bands in the IRPD spectrum of the $(OCS)_2^+Ar$ ion, while isomer c2B has only one band in the $2000-2200$ cm^{-1} region. Therefore, the structure of the $(OCS)_2^+$ part in the $(OCS)_2^+Ar$ ion is attributed to isomer c2A. Since the $(OCS)_n^+$ ($n = 3-6$) ions also show these two bands at ~ 2090 and ~ 2120 cm^{-1}, these clusters have an $(OCS)_2^+$ ion core like c2A. The IR bands of the $(OCS)_n^+$ ($n = 3-6$) ions in the $2000-2070$ cm^{-1} region can be assigned to CO stretching vibrations of "solvent" OCS molecules attached to the $(OCS)_2^+$ ion core, because the band positions are very close to that of OCS neutral monomer (2050.5 cm^{-1}).[47] For the $(OCS)_n^+$ cluster ions, the bands of the $(OCS)_2^+$ ion core appear on the higher frequency side of the solvent bands. This is an opposite trend to the case of the $(CO_2)_n^+$ and $(CS_2)_n^+$ clusters, where the dimer ion cores have lower stretching frequencies than those of solvent components.[27,28] The highest-occupied molecular orbital (HOMO) of OCS has an anti-bonding nature

between the carbon and oxygen atoms. Isomer c2A has an electron hole in a MO of $(OCS)_2$ composed of the HOMOs of the two OCS components. As a result, the CO bonds of c2A are stronger than that of neutral OCS, and the CO stretching frequency of the dimer ion core becomes higher than that of the solvent ones. For the $n = 3$ and 4 ions, the solvent bands appear at ~ 2020 cm^{-1}. In the spectrum of the $n = 5$ ion, a new component clearly appears at ~ 2034 cm^{-1}. This component seems to increase its intensity for the $n = 6$ cluster. These results of the solvent bands suggest that the $(OCS)_2^+$ ion core is strongly solvated by two OCS molecules, and that further molecules are more weakly bonded to the $(OCS)_4^+$ ion.

Here, we discuss the structural similarity and dissimilarity for the $(OCS)_n^+$, $(CO_2)_n^+$, and $(CS_2)_n^+$ ions. As mentioned above, the $(OCS)_2^+$ ion has a non-planar, C_2 structure. This is similar to a C_2 structure of the $(CS_2)^+$ ion[27] but is different from a planar, C_{2h} form of the $(CO_2)_2^+$ ion.[28] Figure 4 displays the most stable structures of the $(CO_2)_2^+$, $(OCS)_2^+$, and $(CS_2)_2^+$ ions calculated at the B3LYP/6-311+G* level of theory.[27,28] The intermolecular dihedral angle of the C–S⋯S–C atoms is narrower for the $(OCS)_2^+$ ion (98.8°) than that for the $(CS_2)_2^+$ ion (115.7°). The O⋯O distance of the $(CO_2)_2^+$ ion (2.32 Å) is much shorter than the S⋯S distance of $(OCS)_2^+$ (2.89 Å) and $(CS_2)_2^+$ (2.96 Å). The binding energies are calculated to be 10 283, 9770, and 8012 cm^{-1} for $(CO_2)_2^+$, $(OCS)_2^+$, and $(CS_2)_2^+$, respectively. In larger cluster cations, $(CO_2)_n^+$, $(OCS)_n^+$, and $(CS_2)_n^+$, dimer ion cores are kept,[27,28] but the $(CO_2)_n^+$ cluster ions show alternate change of the $(CO_2)_2^+$ ion core structure between planar C_{2h} and bent C_2 forms as a function of the cluster size.[28]
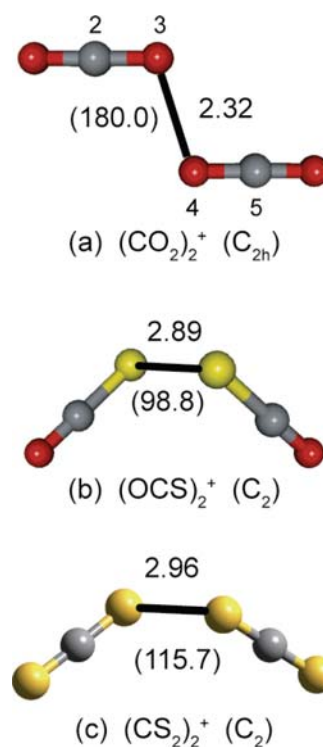
FIG. 4. The most stable structures of the $(CO_2)_2^+$, $(OCS)_2^+$, and $(CS_2)_2^+$ ions calculated at the B3LYP/6-311+G* level. Numbers in the figure represent interatomic distances in Å unit. Numbers in parentheses show dihedral angles (degrees) of atoms 2, 3, 4, and 5 (see Fig. 4(a)).
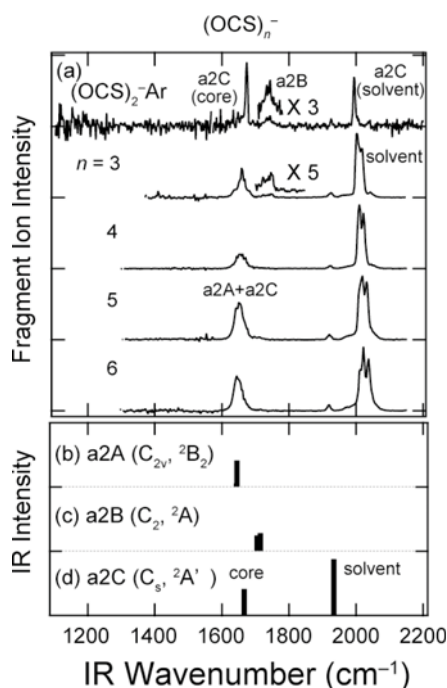
FIG. 5. (a) The IRPD spectra of the $(OCS)_2^-Ar$ and $(OCS)_n^-$ $(n = 3-6)$ ions in the 1100–2200 cm^{-1} region. ((b)–(d)) The IR spectra calculated for geometry-optimized structures of $(OCS)_2^-$. A scaling factor of 0.9689 is employed for the calculated vibrational frequencies.

B. $(OCS)_n^-$

Figure 5(a) shows the IRPD spectra of $(OCS)_2^-Ar$ and $(OCS)_n^-$ $(n = 3-6)$ in the 1100–2200 cm^{-1} region. In the spectrum of the $(OCS)_2^-Ar$ ion, two strong bands appear at 1994 and 1674 cm^{-1} with two weak components at 1734 and 1744 cm^{-1}. The $(OCS)_3^-$ ion also shows weak absorption at ~1740 cm^{-1}, but no band is seen in the $n = 4-6$ clusters around there. For the $(OCS)_n^-$ $(n = 3-6)$ cluster anions, two strong bands are observed at ~1660 and ~2020 cm^{-1}. The intensity of the ~1660 cm^{-1} band relative to that of the ~2020 cm^{-1} one becomes weaker with increasing the size from $n = 2$ to 4, but it suddenly increases at $n = 5$ and 6. Weak bands at ~1900 cm^{-1} are ascribed to the combination band $(2\nu_2 + \nu_1)$ of "solvent" OCS molecules.[47]

The spectral features of the $(OCS)_n^-$ clusters described above can be attributed to the coexistence of three isomers. Figure 6 displays the geometry-optimized structure of the $(OCS)_2^-$ ion at the B3LYP/6-311+G(d) level of theory. Isomer a2A (Fig. 6(a)) is the most stable structure with C_{2v} symmetry and $^2B_2$ electronic state. The negative charge is delocalized over the dimer, and the intermolecular distance is as short as 1.56 Å. The second most stable structure is a2B in Fig. 6(b) (C_2 symmetry). Isomer a2B has ^2A electronic state, which does not correlate with the $^2B_2$ electronic state of isomer a2A. These isomers were reported in the previous study.[36] Isomer a2C is another isomer, having a monomer-ion core structure; 89% of the negative charge is localized in one OCS component, and the other one is bonded to the ion core at the sulfur end as a solvent molecule. The IR spectra calculated for these $(OCS)_2^-$ isomer are compared with the IRPD spectrum of the $(OCS)_2^-Ar$ ion in Fig. 5. Isomer a2A has two closely located bands at 1645 and 1643 cm^{-1}. Also for isomer a2B, there are
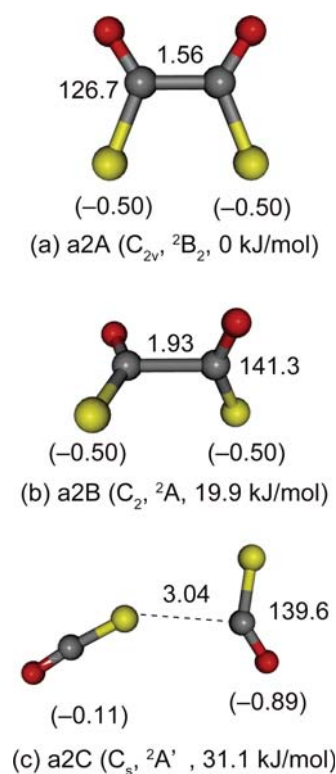
FIG. 6. Optimized structures of the $(OCS)_2^-$ ion. Numbers in the figure show interatomic distances and O–C–S angles. Numbers in parentheses are the Mulliken charge distribution on the constituent molecules. The energy values show the total energy relative to that of the most stable form (a2A). The values are corrected by the zero-point vibrational energy.

two bands at 1715 and 1705 cm^{-1}. The IR spectrum of isomer a2C shows two bands at 1934 and 1667 cm^{-1}. Comparing the IRPD spectrum of the $(OCS)_2^-Ar$ ion with the calculated IR spectra, we assign the structure of the $(OCS)_2^-$ part in the $(OCS)_2^-Ar$ ion to isomer a2C, because the IR spectrum of a2C well reproduces the IRPD spectrum of the $(OCS)_2^-Ar$ ion. The 1934 cm^{-1} and 1667 cm^{-1} bands of isomer a2C are the CO stretching vibrations of solvent OCS and OCS$^-$ anion core, respectively. The weaker components around 1740 cm^{-1} are due to isomer a2B on the basis of the relative band position for isomers a2A–a2C around 1660 cm^{-1}. The spectral features around 2020 cm^{-1} in the $n = 3-6$ spectra can be assigned to solvent OCS components. The attachment of solvent OCS molecules will increase the intensity of the band at ~2020 cm^{-1} relative to the bands of the ion core, as seen for the $(OCS)_n^+$ cation clusters, if the same anion core species is kept over the cluster size. Figure 7 shows the IR absorption intensity of solvent components relative to that of ion core, which is obtained from the IRPD spectra in Figs. 2 and 5. In the case of the cation clusters, a linear trend of the solvent intensity against the cluster size is clearly observed for $n = 2-6$. For the anion clusters, a linear trend can be seen also for the $n = 2-4$ clusters. This suggests that an OCS$^-$ core form like isomer a2C is kept for the $n = 2-4$ ions. In addition, an $(OCS)_2^-$ core form like a2B, which has C_2 symmetry and ^2A electronic state, coexists as a minor isomer for the $n = 2$ and 3 clusters. In contrast, the sudden change in the relative intensity between $n = 4$ and 5 indicates the appearance of different ion-core forms for $n = 5$ and 6. The most probable candidate of the
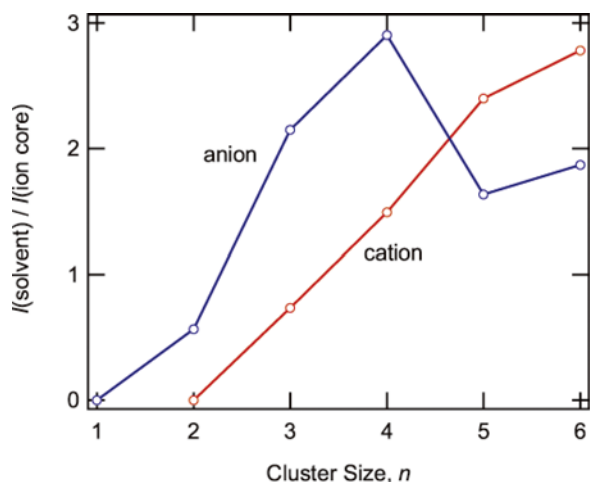
FIG. 7. IR absorption intensity of solvent components relative to that of the ion cores. In order to obtain the intensity of the solvent, cation core, and anion core components, the intensity of the IRPD spectra is integrated in the 1970–2070, 2080–2150, and 1590–1700 cm^{-1} regions, respectively.

FIG. 8. Schematic potential energy surfaces for $(OCS)_2^-$ anion.

ion core is isomer a2A, which has C_{2v} symmetry and $^2B_2$ electronic state (Fig. 6(a)). This isomer has the CO stretching bands at 1643 and 1645 cm^{-1} as seen in Fig. 5(b). The sudden change of the relative intensity of the ~1660 cm^{-1} band at $n = 5$ is probably due to the increase of isomers having an a2A-like ion core. Since the CO stretching bands of a2A and a2C are located closely, the ~1660 cm^{-1} component of the $n = 5$ and 6 spectra can be assigned to both of a2A and a2C. These assignments of the $(OCS)_n^-$ clusters are quite consistent with the previous studies on photochemistry and photoelectron spectroscopy of the $(OCS)_n^-$ anions. The electronic structure of the $(OCS)_n^-$ clusters has been extensively studied by Sanov and coworkers.[36–38] They suggested the coexistence of monomer-based (OCS$^-$ ion core) and dimer-based ($(OCS)_2^-$ ion core) clusters for the $(OCS)_n^-$ ions. In addition, the results of photochemistry showed that the importance of the a2B-ion core structure against the a2A-ion core form decreases with increasing the cluster size.

The electronic and geometric structures of the $(OCS)_n^-$, $(CO_2)_n^-$, and $(CS_2)_n^-$ ions are much more complicated than the cluster cations. It depends highly on the ion source condition, cluster size, and sometimes experimental methods. One difference of the CO_2 system from OCS and CS_2 is that CO_2 monomer has a negative EA.[16] The photoelectron and IRPD studies showed that the $(CO_2)_2^-$ ion has a symmetric form with the negative charge delocalized over the dimer;[16,20] quantum chemical calculations indicated that the $(CO_2)_2^-$ ion has D_{2d} symmetry.[21,48] The $(CO_2)_2^-$ dimer core exists in the $(CO_2)_{3-6}^-$ clusters.[16] The $(CS_2)_n^-$ anions have much more complicated stories. Photoelectron and photodissociation spectroscopy of the $(CS_2)_n^-$ cluster anions suggested the coexistence of electronic isomers with a CS_2^- monomer or $(CS_2)_2^-$ dimer ion core.[39–42,44,45] In contrast, our IRPD study of the $(CS_2)_{3-8}^-$ clusters suggested a CS_2^- monomer ion core form.[27] Very recently, Sanov and coworkers clearly showed the definitive evidence of the electronic and geometric structure of $(CS_2)_2^-$ by IRPD spectroscopy with a temperature-controlled ion trap and a free electron laser.[33] Their IRPD spectra are ascribed to three isomers: one CS_2^- ion core structure with C_s symmetry
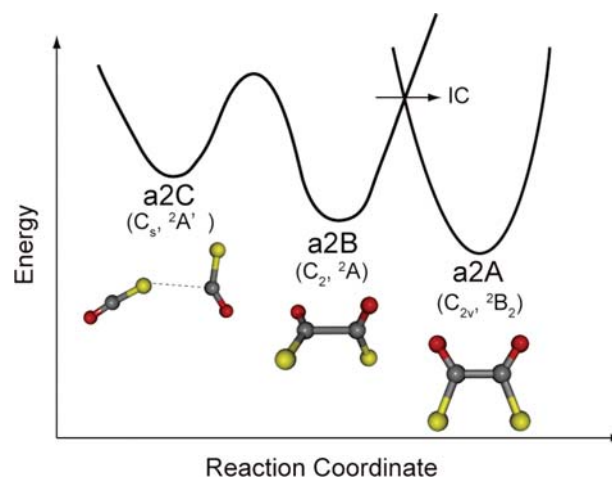
and two symmetric forms with D_{2d} symmetry and $^2A_1$ state or with C_{2v} symmetry and $^2B_1$ state. In the supersonic expansion, the C_s structure is formed predominantly, but it is relaxed to the other D_{2d} or C_{2v} conformer in the ion trap.[33] For the $(OCS)_n^-$ cluster anions, photoelectron and photodissociation experiments showed the coexistence of isomers with OCS$^-$ or $(OCS)_2^-$ ion core.[36–38] The present study shows that three isomers coexist for $(OCS)_n^-$: a2A (C_{2v}, $^2B_2$), a2B (C_2, ^2A), and a2C (C_s, $^2A'$). The common forms for the CO_2, OCS, and CS_2 dimer anions are the twisted D_{2d} forms of $(CO_2)_2^-$ and $(CS_2)_2^-$, and the C_2 (a2B) form of $(OCS)_2^-$. The $(CS_2)_2^-$ and $(OCS)_2^-$ dimer anions have the C_{2v} isomers but different electronic states ($^2B_1$ and $^2B_2$, respectively). In addition, in the case of the $(CS_2)_2^-$ ion, the C_{2v} structure with $^2B_2$ state was found as a minor isomer in the IRPD spectra.[33]

On the basis of the above study of $(CS_2)_2^-$ by Sanov *et al.*, we can draw similar potential energy surfaces of $(OCS)_2^-$ (Fig. 8). The potential energy surface of a2A (C_{2v}, $^2B_2$) does not correlate to that of a2B (C_2, ^2A) and a2C (C_s, $^2A'$). Similar to the case of $(CS_2)_2^-$, the OCS cluster anions produced in the supersonic expansion are kinetically trapped in the OCS$^-$ core form (isomer a2C), indicating the existence of a high potential barrier between the OCS$^-$ core and $(OCS)_2^-$ core forms. Only a small amount of the OCS cluster anions can overcome the barrier, forming isomer a2B. In addition, the internal conversion (IC) should occur to form isomer a2A. As seen in Fig. 5, the larger clusters ($n = 5$ and 6) have a2A, rather than a2B. Hence, the internal conversion occurs effectively for larger clusters, probably due to the symmetry reduction induced by the solvation of OCS molecules.

IV. CONCLUSION

We investigate the structure of the $(OCS)_n^+$ and $(OCS)_n^-$ cluster ions with IRPD spectroscopy in the 1000–2300 cm^{-1} region. The $(OCS)_n^+$ cluster cations have a dimer ion core structure; the cation core forms a semi-covalent bond between the sulfur ends and has C_2 symmetry. The structure of the $(OCS)_2^+$ ion core is similar to the $(CS_2)_2^+$ ion with C_2 symmetry but different from the $(CO_2)_2^+$ ion with C_{2h} symmetry. For the $(OCS)_n^-$ cluster anions, the OCS$^-$ core structure coexists

with the $(OCS)_2^-$ core forms over the cluster range of $n = 2$–6. In the $(OCS)_2^-$ and $(OCS)_3^-$ clusters, the $(OCS)_2^-$ ion core has C_2 symmetry and ^2A electronic state. For the cluster anions larger than $n = 4$, the dimer ion core belongs to C_{2v} symmetry with $^2B_2$ electronic state.

ACKNOWLEDGMENTS

[1] F. H. Field, P. Hamlet, and W. F. Libby, J. Am. Chem. Soc. **91**, 2839–2842 (1969).
[2] M. Meot-Ner, P. Hamlet, E. P. Hunter, and F. H. Field, J. Am. Chem. Soc. **100**, 5466–5471 (1978).
[3] M. Meot-Ner, J. Phys. Chem. **84**, 2724–2728 (1980).
[4] K. Hiraoka, S. Fujimaki, K. Aruga, and S. Yamabe, J. Chem. Phys. **95**, 8413–8418 (1991).
[5] B. Badger and B. Brocklehurst, Nature **219**, 263 (1968).
[6] T. Shida and W. H. Hamill, J. Chem. Phys. **44**, 4372–4377 (1966).
[7] I. A. Shkrob, M. C. Sauer, C. D. Jonah, and K. Takahashi, J. Phys. Chem. A **106**, 11855–11870 (2002).
[8] M. F. Jarrold, A. J. Illies, and M. T. Bowers, J. Chem. Phys. **79**, 6086–6096 (1983).
[9] M. F. Jarrold, A. J. Illies, and M. T. Bowers, J. Chem. Phys. **81**, 214–221 (1984).
[10] A. J. Illies, M. F. Jarrold, W. Wagner-Redeker, and M. T. Bowers, J. Phys. Chem. **88**, 5204–5209 (1984).
[11] M. F. Jarrold, A. J. Illies, and M. T. Bowers, J. Chem. Phys. **82**, 1832–1840 (1985).
[12] J. T. Snodgrass, R. C. Dunbar, and M. T. Bowers, J. Phys. Chem. **94**, 3648–3651 (1990).
[13] K. Ohashi and N. Nishi, J. Chem. Phys. **95**, 4002–4009 (1991).
[14] K. Ohashi and N. Nishi, J. Phys. Chem. **96**, 2931–2932 (1992).
[15] M. J. DeLuca, B. Niu, and M. A. Johnson, J. Chem. Phys. **88**, 5857–5863 (1988).
[16] T. Tsukuda, M. A. Johnson, and T. Nagata, Chem. Phys. Lett. **268**, 429–433 (1997).
[17] R. Mabbs, E. Surber, L. Velarde, and A. Sanov, J. Chem. Phys. **120**, 5148–5154 (2004).
[18] J. K. Song, N. K. Lee, J. H. Kim, S. Y. Han, and S. K. Kim, J. Chem. Phys. **119**, 3071–3077 (2003).
[19] R. Nakanishi, A. Muraoka, and T. Nagata, Chem. Phys. Lett. **427**, 56–61 (2006).
[20] J. W. Shin, N. I. Hammer, M. A. Johnson, H. Schneider, A. Glöß, and J. M. Weber, J. Phys. Chem. A **109**, 3146–3152 (2005).
[21] M. Saeki, T. Tsukuda, and T. Nagata, Chem. Phys. Lett. **340**, 376–384 (2001).
[22] K. Ohashi, H. Izutsu, Y. Inokuchi, K. Hino, N. Nishi, and H. Sekiya, Chem. Phys. Lett. **321**, 406–410 (2000).
[23] Y. Inokuchi and N. Nishi, J. Chem. Phys. **114**, 7059–7065 (2001).
[24] Y. Inokuchi, K. Ohashi, H. Sekiya, and N. Nishi, J. Chem. Phys. **117**, 10648–10653 (2002).
[25] A. Muraoka, Y. Inokuchi, N. Nishi, and T. Nagata, J. Chem. Phys. **122**, 094303 (2005).
[26] A. Muraoka, Y. Inokuchi, and T. Nagata, J. Phys. Chem. A **112**, 4906–4913 (2008).
[27] Y. Kobayashi, Y. Inokuchi, and T. Ebata, J. Chem. Phys. **128**, 164319 (2008).
[28] Y. Inokuchi, A. Muraoka, T. Nagata, and T. Ebata, J. Chem. Phys. **129**, 044308 (2008).
[29] Y. Inokuchi, Y. Kobayashi, A. Muraoka, T. Nagata, and T. Ebata, J. Chem. Phys. **130**, 154304 (2009).
[30] A. Muraoka, Y. Inokuchi, N. I. Hammer, J.-W. Shin, M. A. Johnson, and T. Nagata, J. Phys. Chem. A **113**, 8942–8948 (2009).
[31] Y. Inokuchi, R. Matsushima, Y. Kobayashi, and T. Ebata, J. Chem. Phys. **131**, 044325 (2009).
[32] R. Matsushima, T. Ebata, and Y. Inokuchi, J. Phys. Chem. A **114**, 11037–11042 (2010).
[33] D. J. Goebbert, T. Wende, L. Jiang, G. Meijer, A. Sanov, and K. R. Asmis, J. Phys. Chem. Lett. **1**, 2465–2469 (2010).
[34] K. Hiraoka, K. Fujita, M. Ishida, K. Hiizumi, F. Nakagawa, A. Wada, S. Yamabe, and N. Tsuchida, J. Am. Soc. Mass Spectrom. **16**, 1760–1771 (2005).
[35] T. Kondow and K. Mitsuke, J. Chem. Phys. **83**, 2612–2613 (1985).
[36] A. Sanov, S. Nandi, K. D. Jordan, and W. C. Lineberger, J. Chem. Phys. **109**, 1264–1270 (1998).
[37] E. Surber and A. Sanov, J. Chem. Phys. **118**, 9192–9200 (2003).
[38] E. Surber and A. Sanov, Phys. Rev. Lett. **90**, 093001 (2003).
[39] T. Tsukuda, T. Hirose, and T. Nagata, Chem. Phys. Lett. **279**, 179–184 (1997).
[40] T. Maeyama, T. Oikawa, T. Tsumura, and N. Mikami, J. Chem. Phys. **108**, 1368–1376 (1998).
[41] R. Mabbs, E. Surber, and A. Sanov, Chem. Phys. Lett. **381**, 479–485 (2003).
[42] A. Sanov, W. C. Lineberger, and K. D. Jordan, J. Phys. Chem. A **102**, 2509–2511 (1998).
[43] T. Habteyes, L. Velarde, and A. Sanov, J. Chem. Phys. **130**, 124301 (2009).
[44] T. Habteyes and A. Sanov, J. Chem. Phys. **129**, 244309 (2008).
[45] T. Habteyes, L. Velarde, and A. Sanov, J. Phys. Chem. A **112**, 10134–10140 (2008).
[46] M. J. Frisch et al., GAUSSIAN 03, Revision B.04, Gaussian, Inc., Pittsburgh, PA, 2003.
[47] P. F. Bartunek and E. F. Barker, Phys. Rev. **48**, 516–521 (1935).
[48] M. Saeki, T. Tsukuda, and T. Nagata, Chem. Phys. Lett. **348**, 461–468 (2001).